An Analysis of Coseismic Tilt Changes From an Array in Central California

STUART MCHUGH AND MALCOLM J. S. JOHNSTON

U. S. Geological Survey, Menlo Park, California 94025

Local earthquakes with magnitudes of $\gtrsim 2.5$ and within 20–50 km of tiltmeters along the San Andreas fault typically generate offsets in tilt, tilt seismograms, and impulsive tilt behavior at the time of the earthquake. The amplitudes and azimuths of the coseismic tilt offsets from local earthquakes observed at a small array of four instruments approximately 30 km south of Hollister, California, are compared to the amplitudes and azimuths predicted by a rectangular source, elastic half-space dislocation model. Almost all observed coseismic offset amplitudes are 1–3 orders of magnitude larger than the predicted amplitudes. The predicted offset azimuths also are not in agreement with the observed azimuths. There is neither a uniform method of scaling the predicted amplitudes nor a constant rotation that may be applied to the predicted azimuths that will consistently reproduce the observed offsets. Errors in hypocenter location and fault plane orientation are not sufficient to explain the discrepancies between observations and predictions. Similar results occur for teleseismic earthquakes. A lack of agreement in the observed offset amplitudes across the array indicates that tilt changes are triggered at or near the instrument site by the passage of seismic waves. No significant agreement was obtained between the direction of coseismic tilts and either the secular tilt trends or local geologic features. Triggered movement on near-surface cracks, fractures, and minor faults appears the most viable physical explanation for the observed offsets. Short-base-line near-surface tiltmeters appear inadequate for measuring tilt displacement fields generated by local earthquakes. Deep borehole installations appear necessary for this measurement. Coseismic tilt transients appear to be caused by seismically induced water table perturbations near the tiltmeter site.

INTRODUCTION

The tilt and strain changes associated with earthquakes are of critical importance to models of the earthquake source. Previous work has emphasized the coseismic tilt and strain residual offsets because these are calculable from static dislocation models and are easily identified by coincidence with the earthquake occurrence time. *Press* [1965] reported a strain step of 10^{-8} recorded at Kipapa, Oahu, Hawaii, after the magnitude 8.4, 1964 Alaskan earthquake. This particular strain step was of the amplitude expected from the model presented. There were tilt and strain steps associated with other large teleseisms that were orders of magnitude greater than were expected and were suggested to be caused by geologic complexities or instrumental and/or site effects. *Wideman and Major* [1967] summarize strain step observations for step amplitudes in the range 10^{-4}–10^{-10} recorded at distances up to 10^4 km from the source (nuclear as well as seismic) and event magnitudes from 3.0 to 8.5. They determined a strain step amplitude dependence of $R^{-\alpha}$, $\alpha = \frac{3}{2}$ (R is the epicentral distance). The theoretical analysis by *Ben-Menahem et al.* [1969] suggests that because the predicted amplitude dependence is quadrupole, not radial, α is in the range $1 > \alpha > 6$, depending upon the source-to-station geometry. *McGinley* [1968] analyzed anomalously large strain and tilt step data from four earthquakes and suggested that a model of a weak layer in the lower crust or upper mantle could be used to reproduce some features of the observations if the degree of weakening is quite severe. *Berg and Lutschak* [1973] report tilt steps following local and teleseismic events recorded by the University of Alaska Tripartite Tilt Network that are more than an order of magnitude larger than those expected from *Press*'s [1965] model and tilt step propagation velocities compatible with Rayleigh wave velocities. Although strain steps for the San Fernando earthquake can be fit by a simple half-space dislocation model [*Jungels and Anderson*, 1971], *Alewine and Heaton* [1973] report anomalously large far-field tilt events associated with the February 21, 1973, Point Mugu earthquake that could not be reproduced by using the source parameters in an elastic dislocation model. However, the observed tilts could be satisfactorily fit by the elastic dislocation model if it was assumed that the Point Mugu event caused a small displacement across a fault near the tiltmeters. *King et al.* [1977] report coseismic steps on creep meter records from the San Andreas fault that are 2 orders of magnitude larger than those calculated by using the seismic source parameters. It was suggested that the discrepancy was caused by a contrast in shear modulus across the fault zone.

It would appear that many of these data are reflecting some physical behavior that cannot be adequately explained by the simple static dislocation models. The best test of the half-space model should be for shallow earthquakes at small epicentral distances so that the effects of large-scale regional structures and the earth's sphericity would not be important factors. Also with all earthquakes in approximately the same tectonic regime and geographic location the data should be less influenced by regional trends in source mechanism. Finally, to demonstrate that the data are self-consistent, they should be simultaneously recorded on more than one instrument.

This paper presents the results of an analysis of coseismic tilt changes recorded on four tiltmeters along 7 km of the San Andreas fault, 30 km south of Hollister, California. On these and other instruments there are two main classes of coseismic tilt behavior associated with local earthquakes: tilt offsets and short-term impulsive tilts on which the tilt seismograms are superimposed. The impulsive tilts have fast rise times and a slow decay of up to an hour. This type of dynamic behavior has also been observed on other instrument types (strain meters, gravimeters, etc.) close to the epicentral region but never for teleseismic earthquakes. Since the transients may have a physical mechanism different from the offsets, the two classes of effects will be treated separately.

Paper number 7B0572.

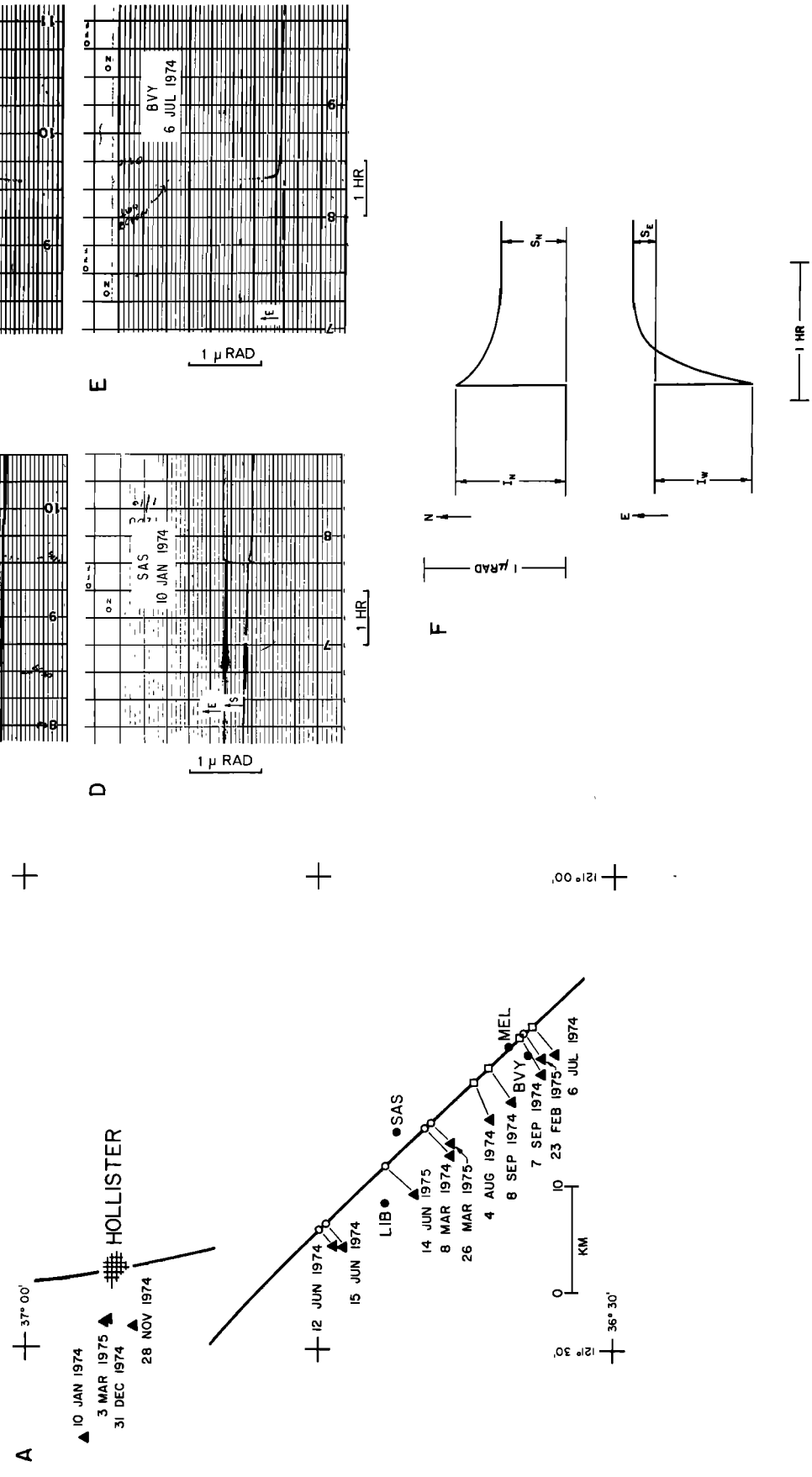

Fig. 1. (*a*) Map of the central San Andreas fault showing instrument sites and epicenter locations for earthquakes used in this analysis. (Group I events are shown by solid triangles, group II events by open circles, and group III events by open squares.) (*b–e*) Copies of some raw records showing time of earthquake occurrence for events and stations used in this analysis. (*f*) Composite of a typical coseismic tilt event associated with a local earthquake without superposition of a 'seismogram.' Amplitude of impulse is indicated by I; amplitude of residual deflection is indicated by S.

TABLE 1. Local Earthquake Data

Event	Date	Time, GMT	Latitude	Longitude	Depth H_0, km	M_L	*ERH*, km	*ERZ*, km
1	Jan. 10, 1974	1122	36°57.08′	121°35.86′	7.84	4.20	0.4	0.6
2	March 8, 1974*	1910	36°38.26′	121°17.51′	4.33	3.14	0.5	0.6
			36°39.5′	121°15.9′				
3	June 12, 1974*	1921	36°44.24′	121°23.41′	6.43	3.70	0.4	0.5
			36°44.9′	121°22.6′				
4	June 15, 1974*	1749	36°43.78′	121°23.64′	6.54	3.28	0.5	0.7
			36°44.6′	121°22.2′				
5	July 6, 1974	0403	36°32.96′	121°11.18′	5.33	3.07	0.5	1.1
			36°34.08′	121°09.36′	2.9	3.1	1.0†	1.0‡
6	Aug. 4, 1974	1503	36°36.19′	121°15.13′	5.61	3.17	0.4	0.6
			36°37.10′	121°12.83′	6.30	3.17	0.2	0.2‡
7	Sept. 7, 1974	2045	36°33.58′	121°12.24′	8.32	3.22	0.4	0.7
			36°34.72′	121°10.11′	6.63	3.21	0.2	0.4‡
8	Sept. 8, 1974	1116	36°35.16′	121°14.20′	7.77	2.86	0.4	0.7
			36°36.35′	121°12.04′	6.95	2.86	0.2	0.2‡
9	Nov. 28, 1974	2301	36°54.95′	121°28.63′	5.51	5.20	0.3	0.9
10	Dec. 31, 1974	2022	36°55.90′	121°28.20′	10.20	4.40	0.4	0.5
11	Feb. 23, 1975*	1724	36°33.60′	121°11.44′	5.00	3.27	0.4	0.5
			36°34.8′	121°10.0′				
12	March 3, 1975	1134	36°55.96′	121°28.38′	7.98	4.30	0.5	0.7
13	March 26, 1975*	2013	36°38.27′	121°16.93′	3.86	3.16	0.5	0.4
			36°39.3′	121°15.7′				
14	June 14, 1975	1256	36°40.11′	121°20.03′	5.61	3.22	0.4	0.6
			36°41.5′	121°18.4′				

M_L is local magnitude; *ERH* and *ERZ* are 1 standard deviation in the horizontal and vertical locations, respectively.

*Group II events (blank rows indicate that values are unchanged).

†*ERH* and *ERZ* estimated from rms value of 0.11 [*Engdahl and Lee*, 1976].

‡*ERH* and *ERZ* estimated are 2 standard deviations (group III events).

INSTRUMENTATION

The U.S. Geological Survey maintains an array of approximately 40 biaxial borehole tiltmeters in central California. Data from four of the longest continuously operating tiltmeters (Libby, LIB; Sage South, SAS; Melendy, MEL; and Bear Valley, BVY in Figure 1*a*) were selected for this investigation.

The instrument resolution is about 10^{-8} rad, although under ideal conditions, somewhat smaller changes can be detected if they occur within a few minutes. The data, passed through a 20-s output filter, are sampled at 8-s intervals. A description of tiltmeter installation and operation is given by *Johnston and Mortensen* [1974].

COSEISMIC TILT OFFSETS ASSOCIATED WITH LOCAL EARTHQUAKES

The residual tilt and strain offsets associated with seismic events have been previously assumed to represent the change in the static field produced by the introduction of a dislocation surface into an elastic medium. Because of the quadrupole nature of the tilt and strain fields a valid test requires a precise estimate of the earthquake source location. For the earthquakes used in this study the influence of possible errors in hypocenter location and fault plane orientation of the local earthquakes on the predicted tilt offsets was determined for each event and each site.

Data from four of the tiltmeters in central California (Figure 1*a*) meet the requirements that (1) generally more than one instrument recorded the same short-period coseismic event for a local earthquake and (2) each tiltmeter recorded several such events in the 18 months studied. Only the five largest earthquakes, ranked by their normalized seismic moment (moment divided by epicentral distance), were chosen for study on tiltmeters within 10 source dimensions of the epicenters. Smaller or more distant earthquakes are less likely to yield tilt changes greater than 10^{-8} rad. Scaling the seismic moment by distance was intended as a crude way of indicating the most significant earthquakes for a particular instrument, although perhaps overestimating their effects (scaling by (distance)$^{-3}$ might be a better choice). Because some of the remaining events were among the five largest at more than one site, the final result was a list of 14 events (Table 1) with local magnitudes M_L between 2.9 and 5.2 and, with very few exceptions, within 50 km of each instrument (Figure 1*a*).

Routine location of the epicenters places the earthquakes west of the San Andreas fault (group I events) probably because of the velocity contrasts between the west side and the east side of the San Andreas fault [*Boore and Hill*, 1973; *Engdahl and Lee*, 1976]. Therefore when the results of *Engdahl and Lee* [1976] were applied, six of the epicenters were relocated onto the fault (group II events). Four of the remaining events (July 6, August 4, September 7, and September 8, 1974) were relocated by W. H. K. Lee, using a computer routine developed for this purpose (group III events). These data are summarized in Table 1 and Figure 1*a*.

The tiltmeter records from each of the four stations corresponding to the earthquake occurrence times (Table 1) were analyzed to determine the effect of the local earthquake on the tilt field. Figures 1*b*–1*e* reproduce examples of local earthquakes recorded by the four central California tiltmeters from the list of events in Table 1. (A complete record of the local earthquakes listed in Table 1 for each of the four sites is given by *McHugh* [1976]. A more detailed discussion of the November 28, 1974, Hollister earthquake is given by *Mortensen and*

TABLE 2. Observed Coseismic Tilt Data

Event	Date	LIB				SAS				MEL				BVY			
		I_A, μrad	I_Z, deg	S_A, μrad	S_Z, deg	τ_I	I_A, μrad	I_Z, deg	S_A, μrad	S_Z, deg	τ_I	I_A, μrad	I_Z, deg	S_A, μrad	S_Z, deg	τ_I	I_A, μrad	I_Z, deg	S_A, μrad	S_Z, deg	τ_I
1	Jan. 10, 1974	0.43	241	0.0	...	2*	0.88	339.	0.07	34.	7						.07	...	0.0	...	0.3*
2	March 8, 1974	0.0	...	0.0	...	0	1.62	135.	≥0.26	135	7						0.04	45.	0.0	...	0.5*
3	June 12, 1974	0.32	266	0.01	243.	2*	0.10	...	0.0	...	1*	≥0.0	...	≥0.0	...		≥0.02	0.0	0.0	...	0.3*
4	June 15, 1974	0.47	270	0.01	90	3*											≥0.80	...	≥0.06	...	33
5	July 6, 1974	0.0	...	0.0	...	0	0.61	325.	0.0	...	3	≥7.07	315*	0.93	288.	25	0.08	21.0	0.0	...	0.3*
6	Aug. 4, 1974						≥1.18	...	≥0.12	...	11	≥0.0	...	≥0.0	...	0	1.25	289.	0.06	351.	2*
7	Sept. 7, 1974	0.0	...	0.0	...	0	≥0.21	...	≥0.0	...	11*	≥0.54	214*	0.63	29.	1*	0.29	0.0	0.0	...	0.3*
8	Sept. 8, 1974	0.04	180.	0.01	45.	0.3*	≥0.09	...	≥0.0	...	2*	0.25	281	0.07	135.	2*	≥1.70	135*	0.0	...	20*
9	Nov. 28, 1974	1.61	249	0.11	326.	14*	2.12	...	0.85	4.0	40	7.92	...	0.29	31.	18*	≥0.09	...	0.0	...	1*
10	Dec. 31, 1974	0.18	227.	0.01	0.0	2*						≥0.15	...	≥0.45	...	3*	≥1.67	98.*	0.07	74.	15
11	Feb. 23, 1975						0.47	187.	0.0	...	2*						0.13	207.	0.0	...	1*
12	March 3, 1975	0.13	243.	0.0	...	2*	0.34	...	0.01	270.	2*						0.06	261.	0.0	...	1*
13	March 26, 1975											0.0	...	0.0	...	0	0.0	...	0.0	...	0
14	June 14, 1975	0.62	115.	0.07	207.	5						0.28	270.	0.25	349.	2*	0.0	...	0.0	...	0

I is impulse, S is residual offset, subscript A is amplitude, subscript Z is azimuth (clockwise from north), and τ_I is the duration of impulses determined to the nearest minute. Values of 0.0 indicate deflections of less than 0.01 μrad. Three centered dots indicate that no azimuth was computed because one tilt component was off scale or was zero or the initial sense of deflection was uncertain. Blank spaces indicate that no data were available.

*Estimated value.

Johnston [1976].) From Figures 1*b*–1*e* it is evident that the main feature of the coseismic short-period tilt change is an initial impulse that decays within minutes to an hour to a residual offset. Neglecting the 'seismogram,' or high-frequency signal, a typical tiltmeter record of a local earthquake is as shown in Figure 1*f*. The amplitude (subscript A) and direction (subscript Z) of the impulse I and residual offset S are summarized in Table 2.

The predicted amplitude and azimuth of the residual offsets were computed for a slip zone that was centered at the earthquake focus in the rectangular dislocation model of *Press* [1965]. The length and vertical extent of the rectangular zone were set equal and were determined from the magnitude-length relation of *Wyss and Brune* [1968]. An upper bound on the coseismic displacement $\bar{u}$ in the model was estimated by substituting the magnitude-moment (M_0) and magnitude–fault plane area (A) relations of *Wyss and Brune* [1968] into $M_0 = \mu\bar{u}A$ [*Aki*, 1966] and assuming that the shear modulus μ is 3×10^{11} dyn/cm^2. (This procedure generates slightly larger displacements than are generated by using the magnitude-moment relation of *Bakun and Bufe* [1975].)

Bounds on the variation in tilt caused by uncertainties in focal location were determined by using the error estimates *ERH* and *ERZ* (Table 1) to vary the source-to-station distance and focal depth, respectively [*McHugh*, 1976]. Figure 2 is a plot of the tilt offset observations for the events listed in Table 1 versus the tilt calculated at the instrument locations from dislocation models of the events. Focal mechanisms of these events indicate strike slip solutions with focal planes from N45°W to N60°W [*Ellsworth*, 1975; *Engdahl and Lee*, 1976]. No substantial difference in this plot obtains if the slip plane is chosen to be N60°W [*McHugh*, 1976].

Results

Amplitude of Coseismic Offset

The observed tilt offset amplitudes as listed in Table 2 and shown in Figure 2 are much greater than the predicted amplitudes. The discrepancy cannot be adequately accounted for by appealing to variations in fault plane orientation or to poor estimates of the source-to-station distance, since the group III events have the best locations presently possible for earthquakes in this region. It is possible but probably unlikely that there is some systematic bias in source strength, instrument calibration, or unknown amplification effects for these sites.

Any systematic bias in amplification would imply uniform scaling between observed and predicted tilt offset amplitudes either for all the data or for the data from each tiltmeter site. Because there is no such consistent trend apparent in the amplitude data, a more complex source of amplification needs to be considered (e.g., it is possible that a shear modulus contrast occurs across the fault zone, as is suggested by *King et al.* [1977]).

If it is assumed that the discrepancy between observed and predicted amplitudes is solely the result of an anomalously low rigidity within the fault zone, it might be expected that uniform scaling would occur for events at a given instrument location after the effects of the source-to-station distance and azimuth have been removed. The results of *McHugh and Johnston* [1977] indicate that surface shear strains within the zone may be amplified by a factor of 2–8 if the shear modulus within the fault zone is an order of magnitude less than it is in the surrounding material and if the source is between 1 and 10 km deep. However, such a model cannot account for either the 2–3 order of magnitude discrepancy observed at the sites or the lack of uniform scaling between observed and predicted offset amplitudes at specific sites (Figure 2).

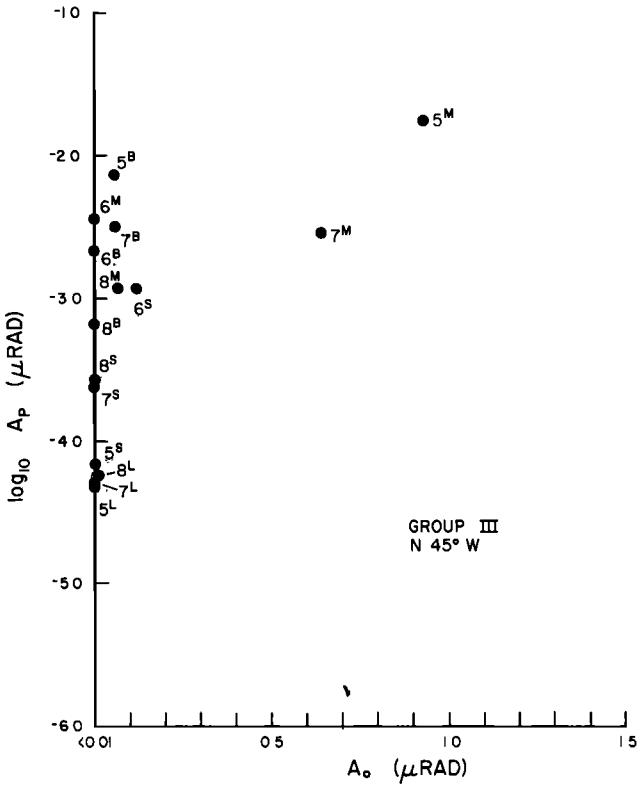

Fig. 2. Logarithm of predicted tilt offset amplitude A for a rectangular source model with a fault plane orientation of N45°W versus observed tilt offset amplitude A at the various stations for the best located earthquakes (group III events). Numbers 5–8 refer to the earthquakes in Table 1; superscripts refer to stations (L is LIB, S is SAS, M is MEL, and B is BVY).

Azimuth of Coseismic Offset

The effect of uncertainties in focal location on the predicted azimuths of the tilt offsets was estimated by using the *ERH* and *ERZ* values in Table 1 to vary the position of the event. Figures 3*a*–3*d* are polar histograms of the differences in tilt offset azimuth between observations and predictions. The radius of the histogram would be a maximum at 0° and of zero length elsewhere if there were (1) no uncertainty in focal location and (2) perfect correspondence between observations and predictions using the source parameters in the half-space model. The distribution of differences in azimuth for group I events, if a fault plane orientation of N45°W is assumed (the average for this region [*Ellsworth*, 1975]), is shown in Figure 3*a*, and that for group II and group III events with a fault plane orientation of N45°W in Figure 3*b*. If Figure 3*a* is compared with Figure 3*b*, it is seen that errors in focal location are insufficient to explain the discrepancy between observations and predictions. Rotations in fault plane orientation from N45°W for group III events (Figure 3*c*) to N60°W (Figure 3*d*), when the rotations are applied uniformly to the group III events, are also insufficient to explain the discrepancy.

A similar study has been made of coseismic tilt offsets associated with teleseisms. These data are reported in the appendix and indicate that (1) the offsets do not have uniform amplitude at all tilt sites as would be expected if they were related to the source and (2) the offsets are also orders of magnitude larger than were expected.

If the tilt steps cannot be explained by dislocations at the earthquake source, it is possible, as was suggested by *Stacey and Rynn* [1970], that they are in the sense of the regional and local secular tilts and are triggered by the passage of seismic waves. This question is discussed in the appendix, and the simplest tests indicate that this does not seem to be the case for these data.

The possibility still remains that the tilt offsets from these near-free surface installations are secondary tilts due to movement on cracks, fractures, and minor or nearby faults such as proposed by *Alewine and Heaton* [1973] for the Point Mugu earthquake. An appeal to this mechanism is somewhat unsatisfactory, since it is always possible to find or propose a fault for which slip and slip dimensions can be chosen that will produce tilts that fit the observations. However, this does appear by default to be the best explanation for the observed tilt offsets. If so, tilt offsets measured on short-base-line tiltmeters on or near the earth's surface will be of little use for earthquake source studies. In any case, determination of the existence and relative importance of these effects is still necessary and is possible with data from recently installed dense arrays in selected locations.

TILT IMPULSES

The observed tilt impulse response with local earthquakes (Table 2) has not been previously discussed, and its physical mechanism is unclear. Since the observed duration of a few minutes up to an hour greatly exceeds the inherent time constant of the tiltmeter, it does appear unlikely that the impulse on the tiltmeter with local earthquakes is of instrumental origin. The free period of the bubble level detector is about 1 s, and the impulse and residual offset are observed whether or not the 20-s filter is in operation. It is conceivable that nonlinear amplifiers could generate a transient response under overload during a large earthquake; however, most observations are for small earthquakes, and the impulse duration is generally much longer than the local earthquake coda at the tiltmeter site. Further, the impulse response is not observed for larger teleseismic events, nuclear explosions, local explosions, or impulsive surface loads within a few meters of the tiltmeter.

The primary differences between the tiltmeter response of local earthquakes and that of teleseismic earthquakes are that (1) the local earthquake tilt seismogram is richer in higher frequencies, (2) the teleseismic arrivals are closer to vertical incidence, and (3) the teleseismic surface waves have longer duration and larger amplitudes. The impulse does occur simultaneously with the earthquake, and some relation of the impulse to the seismic wave parameters might be expected.

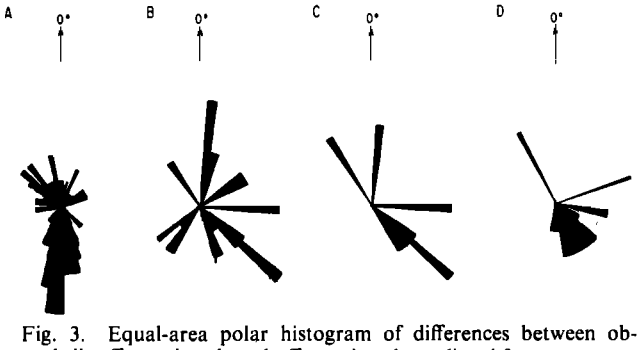

Fig. 3. Equal-area polar histogram of differences between observed tilt offset azimuth and offset azimuth predicted from rectangular source model. Radius of the histogram is proportional to the number of differences in the angular range specified. Fault plane orientations are (*a*) N45°W (group I events), (*b*) N45°W (group II and group III events), (*c*) N45°W (group III events), and (*d*) N60°W (group III events).

Simple checks of the impulse vectors with the seismic radiation pattern (sense of first arrival, P and S amplitudes, etc.) and quasi-static tilt fields produced by dislocations at the earthquake source have failed to demonstrate any direct first-order relation. There is also no apparent relation to the direction of secular tilts, although there may be some indications of geometric and geologic influence. The impulse azimuths at LIB, MEL, and BVY tend to have a westward component for events north of those sites.

The impulses can be modeled by propagating displacement on a nearby secondary fault. However, since the secondary displacement must start quite close to the tiltmeter to produce the rapid onset and since it is unlikely that there is a secondary fault responding with the same form but different sign for different earthquakes, it is hard to justify using this approach.

The form is the most consistent feature of the impulse. A nonlinear soil response to the arrival of the seismic energy implies that the duration of the coseismic tilt change should be comparable to the earthquake coda (i.e., 40–400 s for these local earthquakes). This effect is unlikely to be responsible for coseismic tilt changes with durations of more than 10–15 min. Time dependent strains associated with the diffusion of fluids in porous media following an incremental stress have the same general form [*Booker*, 1974; *Rice and Cleary*, 1976]. If such an effect occurred at the earthquake source, the decay times for the same event would be the same at different sites, and the amplitude should fall off with distance from the source. This is not the case. However, it is possible that time dependent strains from local pore fluid movements are induced near the tiltmeter site by short-period seismic waves. These could produce impulses of the same form but with slightly different decay times as observed.

During and following the 1964 Alaskan earthquake, monitored wells throughout the United States showed level changes similar in form to the tilt impulses [*Cooper et al.*, 1968]. Well level records from a well at the Cienega Winery in the same region as that where the tiltmeters are installed show coseismic signals of the same form but with longer duration [*Johnson*, 1973], and well records near the San Fernando earthquake also show an impulsive onset with a slow decay determined presumably by the near-field diffusion time constant [*Waananen and Moyle*, 1971].

Conclusions

For this analysis of 17 tilt offsets associated with 14 local earthquakes the observed coseismic tilt offset amplitudes are 1–3 orders of magnitude larger than those expected from a rectangular source, elastic half-space dislocation model of the earthquake source. The observed offset azimuths also do not agree with those predicted by the model. Errors in hypocenter location or fault plane orientation are not sufficient to explain the discrepancy. The magnitude of the discrepancy between observed and predicted tilt offset amplitudes might imply a modulus contrast of more than 1 order of magnitude. However, this appears unlikely, since the lack of uniform scaling between observed and predicted offset amplitudes at specific sites requires any modulus contrast effect to operate quite differently from event to event.

Although triggered movement on nearby cracks, fractures, and minor faults, probably related to continuing fault zone evolution and not to the source of a particular seismic event, is not easily quantified, it appears to be the best explanation of these observed coseismic tilt offsets. This implies that similar tilt and strain offsets measured on short-base-line instruments near the earth's surface will be of limited use in source mechanism studies. Installation in deep boreholes at depths of more than ½ km, where local cracks and fractures are closed by lithostatic pressure, may give more meaningful results. With the use of a longer-base-line tiltmeter, local near-surface effects should be of less importance, although other problems may be encountered.

Tilt steps associated with teleseisms appear also to be a result of strain changes triggered by the surface waves, since the amplitudes on different tiltmeters in the array (~5-km separation) can vary by more than an order of magnitude.

Coseismic tilt transients observed with most local earthquakes have the form and amplitude of time dependent strains caused by seismically induced fluid movements near the tiltmeter site, reflecting perturbations in the water table, or local aquifers. In this region the water table is generally not more than a few tens of meters beneath the instruments.

Appendix

An extended version of this paper that includes data on and a discussion of coseismic tilt offsets associated with teleseisms and a comparison of tilt offset directions with the secular tilts appears in a supplement.[1] These data show the following:

1. Offsets associated with teleseisms are also 1–3 orders of magnitude larger than those expected from elastic dislocation models.
2. These offsets do not have uniform amplitude at all sites as would be expected if they were related to the earthquake source.
3. The tilt offset directions apparently do not result from triggering of local secular strain conditions, nor are they clearly related to local geologic features.

References

Aki, K., Generation and propagation of G waves from the Niigata earthquake of June 16, 1964, 2, Estimation of earthquake moment, released energy, and stress-strain drops from the G wave spectrum, *Bull. Earthquake Res. Inst. Tokyo Univ., 44*, 73–88, 1966.

Alewine, R. W., III, and T. H. Heaton, Tilts associated with the Pt. Mugu earthquake, Proceedings of the Conference on Tectonic Problems of the San Andreas Fault System, *Stanford Univ. Publ. Univ. Ser. Geol., 13*, 94–103, 1973.

Bakun, W. H., and C. Bufe, Shear wave attenuation along the San Andreas fault zone in central California, *Bull. Seismol. Soc. Amer., 65*, 439–459, 1975.

Ben-Menahem, A., S. J. Singh, and F. Solomon, Static deformation of a spherical earth model by internal dislocations, *Bull. Seismol. Soc. Amer., 59*, 813–853, 1969.

Berg, E., and W. Lutschak, Crustal tilt fields and propagation velocities associated with earthquakes, *Geophys. J. Roy. Astron. Soc., 35*, 5–29, 1973.

Booker, J. R., Time dependent strain following faulting of a porous medium, *J. Geophys. Res., 79*, 2037–2044, 1974.

Boore, D. M., and D. P. Hill, Wave propagation characteristics in the vicinity of the San Andreas fault system, Proceedings of the Conference on Tectonic Problems of the San Andreas Fault System, *Stanford Univ. Publ. Univ. Ser. Geol., 13*, 215–224, 1973.

Cooper, H. H., et al., The response of well-aquifer systems to seismic waves, in the great Alaska earthquake of 1964, Hydrology, part A, *Publ. 1603*, Nat. Acad. of Sci., Washington, D. C., 1968.

Ellsworth, W. L., Bear Valley, California, earthquake sequence of February–March, 1972, *Bull. Seismol. Soc. Amer., 65*, 483–506, 1975.

Engdahl, E. R., and W. H. K. Lee, Relocation of earthquakes by seismic ray tracing, *J. Geophys. Res., 81*, 4400–4406, 1976.

[1] Supplement is available with entire article on microfiche. Order from American Geophysical Union, 1909 K Street, N. W., Washington, D. C. 20006. Document J77-077. Payment must accompany order.

Johnson, A. G., Pore pressure changes associated with creep events on the San Andreas fault, Ph.D. thesis, Stanford Univ., Stanford, Calif., 1973.

Johnston, M. J. S., and C. E. Mortensen, Tilt precursors before earthquakes on the San Andreas fault, California, *Science, 186,* 1031–1034, 1974.

Jungels, P., and D. L. Anderson, Strains and tilts associated with the San Fernando earthquake, *U.S. Geol. Surv. Prof. Pap., 773,* 77–79, 1971.

King, C.-Y., R. D. Nason, and R. O. Burford, Coseismic steps recorded on creep meters along the San Andreas fault, *J. Geophys. Res., 82,* 1655–1662, 1977.

McGinley, J. R., A comparison of observed permanent tilts and strains due to earthquakes with those calculated from displacement dislocations in elastic earth models, Ph.D. thesis, Calif. Inst. of Technol., Pasadena, 1968.

McHugh, S., Tilt changes of short duration, *Open File Rep. 76-750,* U.S. Geol. Surv., Washington, D. C., 1976.

McHugh, S., and M. J. S. Johnston, Surface shear stress, strain, and shear displacement for screw dislocations in a vertical slab with shear modulus contrast, *Geophys. J., 49,* 715–722, 1977.

Mortensen, C. E., and M. J. S. Johnston, Anomalous tilt preceding the Hollister earthquake of November 28, 1974, *J. Geophys. Res., 81,* 3561–3566, 1976.

Press, F., Displacements, strains, and tilts at teleseismic distances, *J. Geophys. Res., 70,* 2395–2412, 1965.

Rice, J. R., and M. P. Cleary, Some basic stress diffusion solutions for fluid-saturated elastic porous media with compressible constituents, *Rev. Geophys. Space Phys., 14,* 227–241, 1976.

Stacey, F. D., and J. M. W. Rynn, Spurious local effects associated with teleseismic tilts and strains, in *Earthquake Displacement Fields and the Rotation of the Earth,* edited by L. Mansinha et al., pp. 230–233, D. Reidel, Hingham, Mass., 1970.

Waananen, A. O., and W. R. Moyle, Water resources aspects in the San Fernando, California, earthquake of February 9, 1971, *U. S. Geol. Surv. Prof. Pap., 733,* 1971.

Wideman, C. J., and M. W. Major, Strain steps associated with earthquakes, *Bull. Seismol. Soc. Amer., 57,* 1429–1444, 1967.

Wyss, M., and J. N. Brune, Seismic moment, stress, and source dimensions for earthquakes in the California-Nevada region, *J. Geophys. Res., 73,* 4681–4694, 1968.

(Received January 11, 1977;
revised June 6, 1977;
accepted June 6, 1977.)